calculated XRD patterns for the plate-like MoS_2 crystallites containing one and two MoS_2 layers with lateral dimensions of 2.5x2.5 nm (MoS_2 crystallites composed of 8x8x0.5 and 8x8x1 unit cells, respectively).

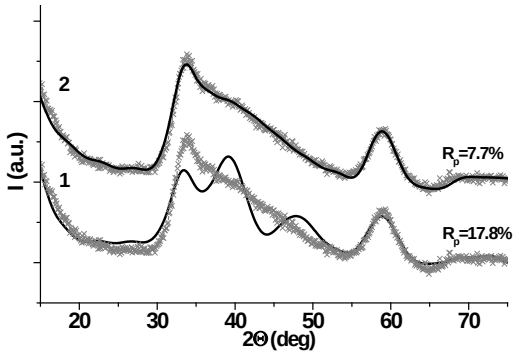

Fig.4. Experimental difference XRD curve of the P-MoS_2/Al_2O_3 catalyst and calculated XRD patterns for MoS_2 crystallites with dimensions of 2.5x2.5x1.2 nm (1) and 2.5x2.5x0.6 nm (2), containing one and two layers along the [001] direction, respectively.

The model of one-layer thick crystallites is more appropriate for describing the experimental XRD pattern. The calculated XRD pattern for the MoS_2 crystallites composed of two layers differs drastically from the experimental one. The lateral dimensions of MoS_2 crystallites of one-layer thickness (slab length) in the P-MoS_2/Al_2O_3 and MoS_2/Al_2O_3 catalysts were refined. The sizes d_{XRD} and corresponding discrepancy factors R_p are listed in Table 1.

The obtained data show that MoS_2 particles in the P-MoS_2/Al_2O_3 catalyst are characterized by a lower average size of coherently scattering domain d_{XRD}. The best fitting results were obtained at the slab sizes of 2.5 and 3.2-3.5 nm for P-MoS_2/Al_2O_3 and MoS_2/Al_2O_3 catalysts, respectively. A comparison of the particle sizes evaluated from XRD and HRTEM data shows a pronounced discrepancy. The dimensions of the coherent scattering domains determined from XRD data are significantly smaller than slab length of MoS_2 determined from HRTEM data (Table 1). The discrepancy is explained by deformation of MoS_2 particles, which leads to breaking coherence. Indeed, the MoS_2 sheets observed in the HRTEM images are curved or folded (Fig. 3). A lower value of d_{XRD} in the case of P-MoS_2/Al_2O_3 catalyst seems to result from a higher degree of deformation of the supported MoS_2 particles.

The results of catalytic testing of the MoS_2/Al_2O_3 and P-MoS_2/Al_2O_3 catalysts in the hydrotreating of RSO/SRGO mixture are presented in the Fig.5-6. Degree of RSO hydrodeoxygenation (Fig.5) was calculated using oxygen content in the raw material (mixture of RSO with SRGO) and in the liquid products measured by means of Vario EL Cube analyzer. The RSO conversion achieved 100% at 320 and 340°C over both catalysts; but P-MoS_2/Al_2O_3 catalyst demonstrated higher HDO activity at 260, 280 and 300°C (Fig.5). P-MoS_2/Al_2O_3 catalyst as well displayed higher activity in HDS of SRGO in comparison with MoS_2/Al_2O_3 catalyst in the whole temperature range (Fig.6).

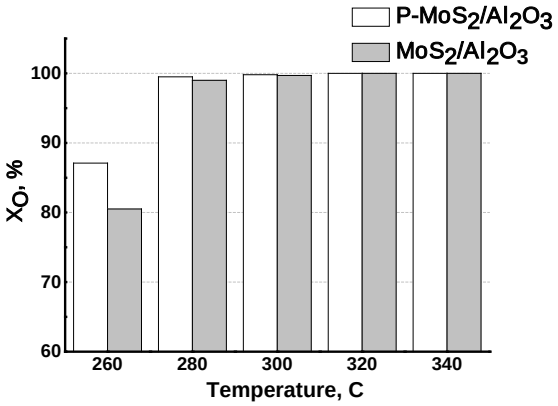

Fig.5. Hydrodeoxygenation activity of P-MoS_2/Al_2O_3 and MoS_2/Al_2O_3 catalysts at different temperatures

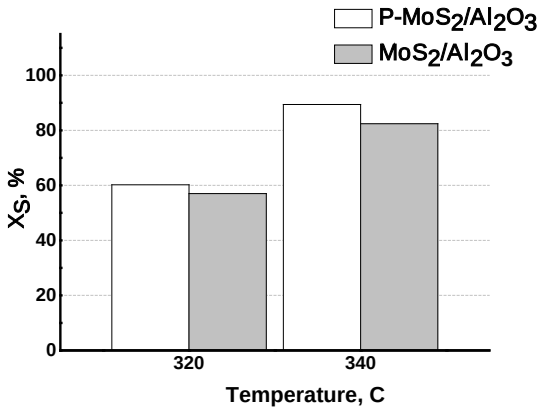

Fig.6. Hydrodesulfurization activity of P-MoS_2/Al_2O_3 and MoS_2/Al_2O_3 catalysts at 320 and 340°C

The selectivity of RSO conversion through HDO or $HDeCO_x$ pathways was evaluated taking gas phase analysis and the results of C_{18} and C_{17} content measurement by means of two-dimensional chromatography.

The typical chromatograms of SRGO and reaction products, obtained during HDO of RSO/SRGO mixture over MoS_2 at 340°C is presented in Fig.7. The quantitative analysis of C_{18} and C_{17} in the reaction products and in the SRGO let

us to calculate the selectivity of octadecane formation that lies within the region 97-99% for both catalysts at whole conversion of RSO (at 320 and 340°C).

The results of CO_x analysis in the exit gas flow confirmed the high selectivity of RSO hydrodeoxygenation though the "direct" HDO route over both catalysts. CO_x content was negligible at 260°C (about 0.04 vol.%) and slightly increased (up to 0.10-0.12 vol.%), with the temperature raising from 260 to 340°C. But the selectivity of $DeCO_x$ pathway calculated from the gas phase analysis did not exceed 3.0% even at 340°C.

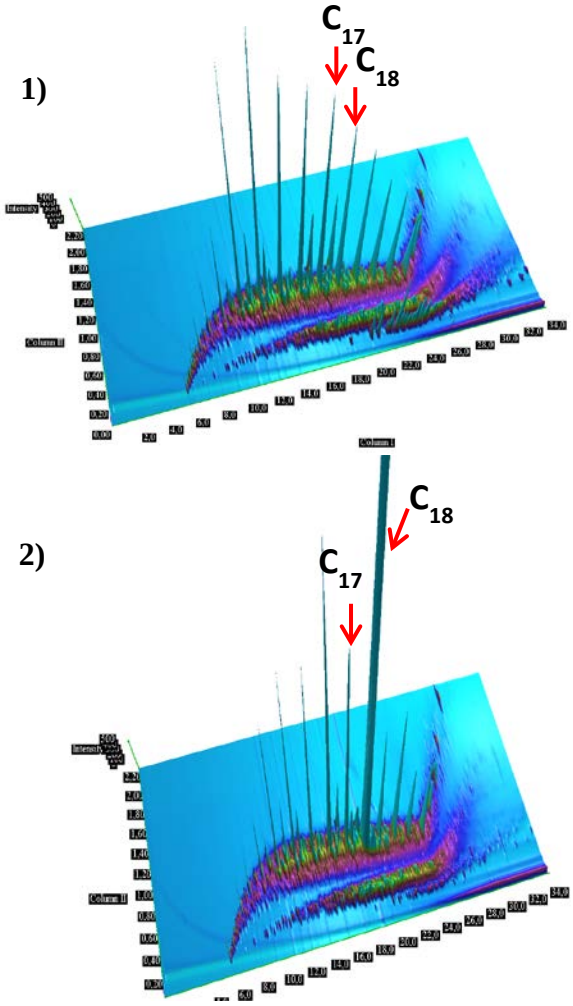

Fig.7. 2D-chromatograms of straight run gas oil (1) and the product obtained (2) in presence of P-MoS_2/Al_2O_3 at 340°C

4 Conclusion

The effect of phosphorus addition on the morphology of MoS_2 phase and catalytic performance of sulfide Mo/Al_2O_3 catalysts in the HDO of rapeseed oil was studied using two different impregnating solutions for preparation of the catalysts. MoS_2/Al_2O_3 catalyst was obtained from solution prepared using MoO_3 and citric acid; the solution prepared from MoO_3, citric acid and H_3PO_4 was used for the P-MoS_2/Al_2O_3 catalyst preparation. The thorough investigation of the sulfide MoS_2/Al_2O_3 and P-MoS_2/Al_2O_3 catalysts with XRD and HRTEM methods led us to conclusion, that despite nearly the same average slab length of MoS_2 particles determined with HRTEM on the surfaces of both catalysts, the MoS_2 particles in the P-MoS_2/Al_2O_3 catalysts are characterized by a lower average size of coherently scattering domain d_{XRD}. A lower value of d_{XRD} in the case of P-MoS_2/Al_2O_3 catalyst seems to result from a higher degree of deformation of the supported MoS_2 particles, maybe due to P incorporation in the MoS_2 slabs. Higher degree of deformation in turn could have been a reason of higher activity of P-MoS_2/Al_2O_3 catalyst in HDO and HDS reactions.

Acknowledgments

The authors would like to thank Dr. Patrushev Yu.V. for analysis and characterization of the products using two-dimensional gas chromatography.

The work was supported by the Ministry of Education and Science of the Russian Federation, project № 14.575.21.0128, unique identification number RFMEFI57517X0128.

References:

[1]Al-Sabawi M., Chen J., Hydroprocessing of biomass-derived oils and their blends with petroleum feedstocks: a review, *Energy & Fuels*, Vol.26, №9, 2012, pp. 5373-5399.

[2] Furimsky E., Hydroprocessing challenges in biofuels production, *Catalysis Today*, Vol.217, 2013, pp. 13-56.

[3] Kubicka D., Tucas V. *Advances in Chemical Engeneering*, Elsevier, Vol.42, 2013.

[4] Mohammad M., Hari T. K., Yaakob Z., Sharma Y. C., Sopian K., Overview on the production of paraffin based-biofuels via catalytic hydrodeoxygenation, *Renewable and Sustainable Energy Reviews*. Vol.22, 2013, pp. 121-132.

[5] Satyarthi J.K., Chiranjeevi T., Gokak D.T., Viswanathan P.S., An overview of catalytic conversion of vegetable oils/fats into middle distillates, *Catalysis Science & Technology*, Vol.3, 2013, pp. 70-80.

[6] Nikul'shin P., Sal'nikov V., Pimerzin A., Eremina Y., Koklyukhin A., Tsvetkov V., Pimerzin A., Co-hydrotreating of straight-run diesel fraction and vegetable oil on Co(Ni)-PMo/Al_2O_3 catalysts , *Petroleum Chemistry*, Vol.56, №1, 2016, pp. 56-61.

[7] Vlasova E. N., Deliy I. V., Nuzhdin A. L., Aleksandrov P. V., Gerasimov E. Y., Aleshina, G. I., Bukhtiyarova, G. A., Catalytic properties of $CoMo/Al_2O_3$ sulfide catalysts in the hydrorefining of straight-run diesel fraction mixed with rapeseed oil, *Kinetics and Catalysis*, Vol.55. №4, 2014, pp. 481-491

[8] Anthonykutty J. M., Linnekoski J. et al., Catalytic upgrading of crude tall oil into a paraffin-rich liquid, *Biomass Conversion and Biorefinery*, Vol.5, №2, 2015, pp. 149-159.

[9] Tóth C., Baladincz P., Hancsók J, Production of biocomponent containing gas oil with the coprocessing of vegetable oil–gas oil mixture, *Topics in Catalysis*, Vol.54, №16-18, 2011, pp. 1084-1093.

[10]Srifa A., Faungnawakij K. et al., Production of bio-hydrogenated diesel by catalytic hydrotreating of palm oil over $NiMoS_2$/gamma-Al_2O_3 catalyst, *Bioresource Technology*, Vol.158, 2014, pp. 81-90.

[11] Kubicka D., Kaluza L., Deoxygenation of vegetable oils over sulfided Ni, Mo and NiMo catalysts, *Applied Catalysis A: General*, Vol.372, №2, 2010, pp. 199-208.

[12] De Brimont M. R. et al., Deoxygenation mechanisms on Ni-promoted MoS_2 bulk catalysts: a combined experimental and theoretical study, *Journal of Catalysis*, Vol.286, 2012, pp. 153-164.

[13] Deliy I. V. et al., Hydrodeoxygenation of methyl palmitate over sulfided Mo/Al_2O_3, $CoMo/Al_2O_3$ and $NiMo/Al_2O_3$ catalysts, *RSC Advances*, Vol.4, №5, 2014, pp. 2242-2250.

[14] Debye P., Scattering from non-crystalline substances, *Ann. Physik.*, Vol. 46, 1915, pp. 809-823.

[15] Guinier A., *X-ray Diffraction in Crystals, Imperfect Crystals and Amorphous Bodies*, Dover, New York, 1994.

[16] Hall B. D., Debye function analysis of structure in diffraction from nanometer-sized particles, *Journal of Applied Physics*, Vol.87, №4, 2000, pp. 1666-1675.

[17] Tsybulya S. V., Yatsenko D. A., X-ray diffraction analysis of ultradisperse systems: The Debye formula, *Journal of Structural Chemistry*, Vol.53, №1, 2012, pp. 150-165.

[18] Yatsenko D. A., Tsybulya S. V., DIANNA (Diffraction Analysis of Nanopowders): Software for structural analysis of ultradisperse systems by X-Ray methods, *Bulletin of the Russian Academy of Sciences: Physics*., Vol.76, №3, 2012, pp. 382-384.